

**HHS PUBLIC ACCESS**

Author manuscript

Neurobiol Aging. Author manuscript; available in PMC 2018 January 01.

Published in final edited form as:

Neurobiol Aging. 2017 January ; 49: 100–108. doi:10.1016/j.neurobiolaging.2016.09.015.**Cortical gray & subcortical white matter associations in Parkinson's disease****N.W. Sterling, Ph.D., M.S.¹, G. Du, M.D., Ph.D.¹, M.M. Lewis, Ph.D.^{1,2}, S. Swavely, M.D.¹, L. Kong, Ph.D.³, M. Styner, Ph.D.⁷, and X. Huang, M.D., Ph.D.^{1,2,5,6,*}**¹Department of Neurology, Pennsylvania State University-Milton S. Hershey Medical Center, Hershey PA 17033, USA²Department of Pharmacology, Pennsylvania State University-Milton S. Hershey Medical Center, Hershey PA 17033, USA³Department of Public Health Sciences, Pennsylvania State University-Milton S. Hershey Medical Center, Hershey PA 17033, USA⁴Department of Radiology, Pennsylvania State University-Milton S. Hershey Medical Center, Hershey PA 17033, USA⁵Department of Neurosurgery, Pennsylvania State University-Milton S. Hershey Medical Center, Hershey PA 17033, USA⁶Department of Kinesiology, Pennsylvania State University-Milton S. Hershey Medical Center, Hershey PA 17033, USA

*Corresponding Author: Xuemei Huang M.D., Ph.D., Departments of Neurology, Neurosurgery, Radiology, Pharmacology, and Kinesiology, Penn State University-Milton S. Hershey Medical Center, H037, 500 University Drive, Hershey, PA 17033-0850, United States, Office phone: 1-717-531-0003, ext. 287082; Fax: 1-717-531-0266; xuemei@psu.edu.

Author Contributions:

Author Name	Email	Contributions
Nicholas W. Sterling	nsterling@hmc.psu.edu	1A, 1B, 1C, 2A, 2B, 2C, 3A, 3B
Guangwei Du	guangweidu@hmc.psu.edu	1A, 1B, 1C, 2A, 2C, 3B
Mechelle M. Lewis	mlewis5@hmc.psu.edu	1A, 1B, 1C, 2C, 3A, 3B
Steven Swavely	steveswavely@gmail.com	1B, 1C, 3B
Lan Kong	lkong@phs.psu.edu	1A, 1B, 1C, 2A, 2B, 2C, 3B
Martin Styner	styner@cs.unc.edu	1A, 1B, 1C, 2C, 3B
Xuemei Huang	xuemei@psu.edu	1A, 1B, 1C, 2A, 2C, 3A, 3B

1. Research project: A. Conception B. Organization C. Execution

2. Statistical Analysis: A. Design B. Execution C. Review & critique

3. Manuscript: A. Writing of first draft B. Review & critique

Conflict of interest disclosures:

Drs. Sterling, Du, Lewis, Kong, Styner, Swavely, and Huang have no conflicts-of-interest relative to this research.

Publisher's Disclaimer: This is a PDF file of an unedited manuscript that has been accepted for publication. As a service to our customers we are providing this early version of the manuscript. The manuscript will undergo copyediting, typesetting, and review of the resulting proof before it is published in its final citable form. Please note that during the production process errors may be discovered which could affect the content, and all legal disclaimers that apply to the journal pertain.

⁷Departments of Computer Science and Psychiatry, University of North Carolina, Chapel Hill, NC 27599, USA

Abstract

Cortical atrophy has been documented in both Parkinson's disease (PD) and healthy aging, but its relationship to changes in subcortical white matter is unknown. This was investigated by obtaining T1- and diffusion-weighted images from 76 PD and 70 controls at baseline, 18-, and 36-months, from which cortical volumes and underlying subcortical white matter axial (AD), radial (RD) diffusivities, and fractional anisotropy (FA) were determined. Twelve of 69 cortical subregions had significant group differences, and for these underlying subcortical white matter was explored. At baseline, higher cortical volumes were significantly correlated with lower underlying subcortical white matter AD, RD, and higher FA ($P < 0.017$) in PD. Longitudinally, higher rates of cortical atrophy in PD were associated with increased rates of change in AD RD, and FA values ($P < 0.0013$) in two subregions explored. The significant gray-white matter associations were not found in controls. Thus, unlike healthy aging, cortical atrophy and subcortical white matter changes may not be independent events in PD.

Keywords

Parkinson's disease; cortical atrophy; white matter; myelin; diffusion tensor imaging

1 INTRODUCTION

Ontogenetically, cortical neurons are born closely to each other in the ventricular zone, and migrate along a common pathway to form cortical columns (Rakic, 1988). The final number of cortical columns and the number of neurons in each column determines the cortical surface area and thickness, respectively (Rakic, 1995). Cortical thickness and surface area are thought to be independent genetically, and may reflect separate processes (Winkler et al., 2010). Cortical volume, however, may be a useful measure to detect overall structural changes during aging or disease processes, since it is the combined property of thickness and surface area. Indeed, loss of cortical volume has been documented both in healthy aging (Abe et al., 2008; Storsve et al., 2014) and Parkinson's disease (PD) (Lewis et al., 2016), although the underlying mechanisms might be different. In healthy aging, dendrite losses and/or shrinkage of larger neurons (Terry et al., 1987) may drive the changes in cortical volume, since the number of cortical neurons is thought to remain relatively constant (Bartzokis et al., 2001; Freeman et al., 2008; Jernigan et al., 2001; Scheibel et al., 1975). In PD, cortical cell losses (Jiang et al., 2012; Ribeiro et al., 2013) may contribute to the loss of cortical volume.

Post-mortem analysis of Lewy pathology has supported the notion that the progression of PD follows a characteristic pattern involving first the brain stem early, and then cortical regions as disease advances (Braak et al., 2003a). The recent discovery that Lewy pathology can spread across neurons has fueled the notion that neuronal disease may spread in a prion-like process (Chu and Kordower, 2015). In addition, it has been suggested that long, thin, and poorly myelinated neurons (such as cortical projection neurons) are preferentially

vulnerable to Lewy pathology (Braak et al., 2006a). Thus, it seems likely that subcortical white matter tracts that contain bidirectional axonal projections from cortical neurons (Singh, 2006) could be an integral part of the PD process. Thus, we hypothesized that the neurodegenerative processes occurring during PD might alter the relationships between cortical gray matter and subcortical white matter. The current study utilized cortical gray matter volume and subcortical white matter tract diffusion measurements, collected longitudinally over 36 months in PD and healthy control subjects, to test this hypothesis.

2 METHODS

2.1 Study subjects

PD (n=76) and control (n=70) subjects having a Mini Mental State Examination score ≥ 26 (Dubois et al., 2007; Goetz et al., 2008a) were selected from a longitudinal cohort study (Table 1). PD patients were recruited from a tertiary movement disorders clinic, and control subjects were recruited from spousal populations and the local community. PD diagnosis was confirmed using published criteria (Hughes et al., 1992). All subjects were free of major and acute medical issues or neurological disorders except PD. All brain images were inspected and deemed free of any major structural abnormalities or motion artifacts. In accordance with the Declaration of Helsinki, written informed consent was obtained for all subjects. The study protocol was approved by the Penn State Hershey Institutional Review Board.

2.2 Clinical information and evaluation

Clinical information and evaluation data were obtained at each visit (baseline, 18-, and 36-months). Hamilton Depression Rating Scale (Hamilton, 1960) and Montreal Cognitive Assessment (Nasreddine et al.) scores were obtained at each visit. In addition, Unified PD Rating Scale (UPDRS) motor scores and Hoehn-Yahr stages were assessed for PD subjects in the “on-medication” state (Fahn and Elton, 1986; Goetz et al., 2008b). Levodopa-equivalent daily dose was calculated according to published criteria (Tomlinson et al., 2010).

2.3 MRI data acquisition

All subjects were scanned using a 3.0 Tesla magnetic resonance scanner (Trio, Siemens Magnetom, Erlangen, Germany, with an 8-channel phased array head coil) at baseline, 18-, and 36-months. A magnetization-prepared rapid acquisition gradient echo sequence was used to obtain T1-weighted images with TR/TE = 1540/2.34, FOV = 256 mm x 256 mm, matrix = 256 x 256, slice thickness = 1 mm (with no gap), slice number = 176, slice selection direction is sagittal. For diffusion tensor imaging, acquisition parameters were as follows: TR/TE=8300/82 ms, b value=1000 s/mm², diffusion gradient directions=42 and 7 b=0 scans, FOV=256 mm x 256 mm, matrix=128 x 128, slice thickness=2 mm (with no gap), and slice number=65, phase encoding direction is axial.

2.4 Structural image processing

T1-weighted brain images were processed automatically using the FreeSurfer (version 5.1.0) longitudinal pipeline (Bernal-Rusiel et al., 2013). Briefly, this pipeline creates unbiased within-subject templates that then were used to initialize image processing (skull stripping,

Talairach transformations, atlas registration, spherical surface maps) for scans at each visit (Fischl and Dale, 2000; Reuter and Fischl, 2011). Cortical volumes were computed by multiplying cortical thickness and surface area at each cortical surface vertex. Gray matter volumes in each cortical region were computed using regional means extracted from cortical parcellations (FreeSurfer's Desikan atlas) (Desikan et al., 2006). Intracranial volume was calculated automatically by FreeSurfer using the method described by Buckner et al. (Buckner et al., 2004).

2.5 Diffusion tensor image processing

Diffusion image quality control and tensor reconstruction was performed using DTIPrep (Neuro Image Research & Analysis Laboratory, University of North Carolina, Chapel Hill, NC USA). This software first checks diffusion weighted images for quality by calculating the inter-slice and inter-image intra-class correlation, and then corrects for the distortions induced by eddy currents and head motion (Liu et al., 2010). Diffusion tensor images subsequently were estimated via weighted least squares (Salvador et al., 2005). Additional quality control was performed by visually inspecting the images for artifacts and directionality. Diffusion tensor images were skull-stripped using brain masks generated from the T1 image segmentation step.

Atlas building was performed using a two-stage process in order to ensure that the overall final atlas was not biased by subject dropout. The first stage involved creation of within-subject atlases using images from each subject's baseline and follow-up images. The second stage involved creation of an overall atlas using the within-subject atlases of all subjects. For creation of both the within-subject and the overall atlases, we utilized the DTIAtlasBuilder program (Neuro Image Research & Analysis Laboratory, University of North Carolina, Chapel Hill, NC USA). This software employs a state-of-the-art image registration pipeline. To generate atlases, affine registration first is applied using the BRAINSFit module within Slicer (Johnson et al., 2007). Second, unbiased diffeomorphic deformations fields are computed using the GreedyAtlas module within AtlasWerks (Joshi et al., 2004). Third, a refinement step is applied via symmetric diffeomorphic registration with the Slicer DTI-Reg module using Advanced Normalization Tools (Avants et al., 2008; Klein et al., 2009). The final step of DTIAtlasBuilder concatenates the transforms of the previous steps to compute the overall transformation of the original diffusion tensor images into the final average diffusion tensor imaging atlas. This allows for mapping between the atlas and the individual diffusion tensor images recorded at each visit without the need for resampling.

For the current study, we chose to use axial diffusivity (thought to be more specific to axonal degeneration), radial diffusivity (thought to correlate inversely with axonal myelination), and fractional anisotropy (FA; thought to reflect overall microstructural integrity) (Aung et al., 2013; Song et al., 2002; Song et al., 2005). We defined several specific regions of interest on the FA map of the average DTI atlas. These regions of interest were chosen specifically for their relation to overlying cortical gray matter. "Overall subcortical white matter" was defined as a region of interest that was generated by first thresholding the overall final atlas image at fractional anisotropy > 0.2 (Supplementary Figure 1). The thresholded mask then was edited manually to exclude white matter in the brainstem, cerebellum, thalamus, and

other gray matter where fractional anisotropy fell beyond the 0.2 threshold level. This final region of interest was used to extract diffusion scalar values of “overall subcortical white matter.” We also examined subcortical white matter diffusion scalars in specific subcortical regions that were named according to the overlying gray matter. This was performed by co-registering a standardized white matter parcellation atlas (JHU-MNI-SS-TypeI) with the overall final atlas, and then mapping the parcellated white matter regions back to the original diffusion tensor images (Oishi et al., 2009).

2.6 Statistical analysis

2.6.1 Group Comparisons—Age and years of education were compared between PD and control subjects using two-sample *t*-tests, whereas gender frequencies were compared using Fisher’s Exact Test. Mini Mental State Exam, Montreal Cognitive Assessment, and Hamilton Depression scores were compared between groups using Wilcoxon Rank-Sum Test. Baseline total and regional cortical gray matter volumes and white matter diffusion measurements were compared using one-way analysis of covariance with adjustment for age, gender, education, and depression scores, with intracranial volume added as a covariate for the gray matter analysis. To limit the probability of false positive findings in our analysis of gray matter-subcortical white matter relationships (see below), we restricted our analyses to cortical areas that had raw $p < 0.05$ in group comparisons between and control subjects (total=12 regions). Rates of annual change in gray matter volumes and white matter diffusion were compared between groups using a linear mixed effects model with random slopes and intercepts and the same covariates as above, with the additional term of years elapsed (since baseline) and the interaction term years elapsed \times group.

2.6.2 Gray matter-subcortical white matter associations—The baseline relationships between gray matter volume and subcortical white matter diffusion were explored using a linear model that included gray matter volume as the dependent variable and the following independent variables: subcortical white matter diffusion scalar, intracranial volume, age, gender, education, Hamilton depression score, and years since diagnosis (as appropriate). To test whether the correlation between gray matter and subcortical white matter depended upon group status (PD vs. control), we performed interaction analyses by adding the additional independent variable of PD (yes/no) \times subcortical white matter diffusion scalar.

Longitudinal data were analyzed by linear regression where the slope of white matter diffusion across all visits (annual rate per subject) was the dependent variable and the independent variable was the slope of gray matter volume across all visits (annual rate per subject). Group differences were assessed using the additional term group \times annual rate of gray matter volume change.

To lessen the likelihood that extreme values and/or non-normally distributed distributions might drive the study results, all cross-sectional comparisons and correlations using imaging measurements were analyzed using multiple linear regression and p-values generated via permutation testing of the model residuals (10,000 iterations) (Anderson and Legendre, 1999; Freedman and Lane, 1983). Raw p-values are reported due to the step-wise nature of

the analysis, however, values that survived correction for multiple comparisons are noted (Benjamini and Hochberg, 1995). For the main hypothesis, we focused on total cortical gray matter volumes and subcortical diffusion properties, corrected for multiple comparisons based on the three diffusion measurements (AD, RD, and FA), and statistical significance was defined as $p < 0.017$. For the explorative analyses, we corrected for multiple comparisons based on the 12 regions of interest and three diffusion measurements, with statistical significance defined as $p < 0.0013$. All analyses were completed using R version 3.1.1 (Bates et al., 2015; R_Core_Team, 2016).

3 RESULTS

3.1 Demographic and clinical characteristics of study subjects at baseline

Compared to controls, PD subjects were significantly older ($p=0.011$), but did not have significant differences either in gender frequency or education (Table 1). PD subjects, however, had lower Mini Mental State Examination ($p=0.024$) and Montreal Cognitive Assessment ($p=0.007$) scores, and higher depression scores ($p<0.0001$) than control subjects. Clinical characteristics of PD subjects are summarized in Table 1.

3.2 Selection of cortical gray matter regions of interest for correlation analyses

Table 2 summarizes the total gray matter volume data, along with the baseline and annual change data for the 12 cortical subregions. As it relates to the primary hypothesis of this work, at baseline PD subjects had lower total cortex volume compared to control subjects ($p=0.006$). We then explored gray matter differences of 69 parcellated regions; this revealed 12 subregions that had significant ($p<0.05$) group differences. We then focused on the total cortical volume-white matter relationship (primary hypothesis), and also explored these 12 subregions to attempt to understand the relationship between cortical subregional gray matter volume and underlying white matter diffusion properties.

Table 3 summarizes the baseline and annual changes of both total subcortical white matter, and the 12 regions of interests that were explored. Several significant effects were seen at baseline, but none of these differences between PD and control subjects survived correction for multiple comparisons either at baseline or longitudinally.

3.3 Correlations of cortical volume and white matter diffusion

At baseline, total cortex volume was correlated negatively with overall subcortical white matter axial and radial diffusivity, and positively with overall subcortical white matter fractional anisotropy in PD, but not in control subjects (Table 4). None of the associations in the 12 studied subregions survived correction for multiple comparisons. The associations seemed to be different in PD compared to controls, with only RD surviving multiple comparison correction ($p=0.011$, Figure 1 and Supplemental Table 1).

Longitudinally, annual loss of total cortex volume was not correlated significantly with the annual increase in subcortical white matter diffusion measurements (Table 5). The exploration of cortical subregions demonstrated that cortical atrophy in the left lateral occipital area was significantly associated with increasing axial and radial diffusivities over

time, and cortical atrophy in the left postcentral region also was significantly associated with increasing fractional anisotropy over time (Table 5, Supplementary Table 2, and Figure 2). The associations were not found in controls.

3.4 Sensitivity analysis using matched PD and control samples

In our prior analysis, we factored in age. To address specifically the possibility that the correlation differences between PD and control subjects were due to age differences between the samples, we performed a sensitivity analysis using 61 PD and 60 control subjects matched on age. There was no significant difference in age ($p=0.493$) or gender ($p=0.474$) between the groups. Baseline overall subcortical white matter radial diffusivity was correlated inversely with total cortical volume in PD subjects ($p=0.0002$), and the correlations were absent in controls ($p=0.804$, interaction $p=0.023$).

4 DISCUSSION

To our knowledge, the current study is the first to investigate the relationship between gray matter atrophy and white matter diffusion properties in PD and healthy controls. The results suggest that cortical gray matter atrophy in PD may be related to microstructural changes of underlying subcortical white matter, a phenomenon not present in healthy controls. Future investigation of the responsible mechanisms is warranted since they may have important implications for understanding PD pathology and its progression.

4.1 Gray matter and white matter changes in PD

Gray matter atrophy in PD has been reported by a number of groups (Hwang et al., 2013; Ibarretxe-Bilbao et al., 2012; Lewis et al., 2016; Pereira et al., 2014; Ramirez-Ruiz et al., 2007; Segura et al., 2014; Song et al., 2011; Tinaz et al., 2011; Zhang et al., 2014), and the current study confirmed these findings in a longitudinal cohort. On the other hand, past research has yielded inconsistent results regarding the extent and nature of white matter involvement in PD. Some studies have suggested that PD subjects have altered subcortical white matter diffusion properties (Auning et al., 2014; Duncan et al., 2015; Gattellaro et al., 2009; Gu et al., 2014; Hattori et al., 2012; Huang et al., 2014; Koshimori et al., 2015) particularly in advanced-stage, cognitively impaired, and depressed patients (Bohnen and Albin, 2011). Conversely, other studies have found none or minimal evidence of altered white matter measures in PD (Ji et al., 2015; Rizzo et al., 2008; Tsukamoto et al., 2012; Worker et al., 2014). The current study falls on the side of those that report altered white matter diffusion properties in several brain regions of non-demented PD subjects. No subcortical white matter diffusion differences, however, survived correction for multiple comparisons. Similarly, although the rate of cortical gray matter volume loss in most cortical regions examined was accelerated significantly in PD compared to control subjects, we found no differences in the rates of white matter diffusion change. This may indicate that the effects of PD on white matter microstructural integrity are weaker than those leading to gray matter atrophy. It also may be that white matter microstructural changes are more difficult to capture via diffusion tensor imaging. Larger sample sizes and more sensitive methods for capturing white matter properties on imaging might be useful in the future.

4.2 The gray-white matter associations in PD

Our findings of a gray matter-white matter association in PD are in agreement with those of Ham et al. (2015), who reported that cortical atrophy was associated with the distribution of white matter hyperintensities in PD. The current study, however, utilized distinct diffusion measures (axial and radial diffusivity, and fractional anisotropy) that provide quantitative measurements of the microstructural properties of subcortical white matter, as opposed to categorical classification of white matter hyperintensities (Ham et al., 2015). In addition, we utilized a spatial approach to pair cortical gray matter areas with underlying subcortical white matter, and included a control cohort for comparison of correlation strengths. It is possible that the observed gray matter-white matter relationships represent separate parallel processes throughout PD progression. This is less likely, however, because we included years-since-diagnosis” as a covariate in the analyses to account for progression effects. Taken together, these findings suggest that degenerative changes in cortical gray matter and subcortical white matter are not necessarily independent phenomena in PD.

4.3 Possible biological mechanisms of the gray-white matter associations in PD

Although there are several possible explanations for the observed gray matter-white matter correlations in PD, the exact mechanism is unknown. The gray matter-white matter associations might be due to the death of the overlying cortical cells resulting in anterograde degeneration of axons in the subcortical white matter (Carrera and Tononi, 2014). This would be consistent with previous reports suggesting that the number of cortical neurons in normal aging remains relatively constant (Freeman et al., 2008; Terry et al., 1987), whereas PD subjects undergo cell losses (Braak et al., 2003b; Fukuda et al., 1999; Jiang et al., 2012). In addition, microstructural damage to subcortical white matter axons might cause cellular changes in the overlying cortical gray matter substrate. This notion is supported by the reported cortical atrophy that is associated with subcortical white matter hyperintensities in both PD (Ham et al., 2015) and non-PD (Seo et al., 2012) populations. Finally, the extent of subcortical white matter myelination may influence cortical neuronal survival in PD. Recent studies have indicated that in PD subjects unmyelinated axons in cardiac nerves accumulate more α -synuclein aggregates (Orimo et al., 2011), and regions with greater myelination during human development are associated with less Lewy deposition (Braak et al., 2006b). Thus, it is possible that greater white matter RD (Figures 1 and 2) may represent less axonal myelination associated with increased vulnerability of overlying cortical gray matter to α -synuclein aggregation or Lewy body deposition.

It is important to note that cortical gray matter volume is known to decrease throughout the lifespan (Abe et al., 2008; Storsve et al., 2014), and subcortical white matter axial and radial diffusivities increase sharply after age 60 (Sexton et al., 2014; Westlye et al., 2010). In normal aging, there is a loss of dendrites in the cortex (Dickstein et al.) and subcortical white matter fibers (Marnier et al., 2003). Consistent with this, the current study found overall cortex atrophy and altered subcortical white matter diffusion over time in both PD and control subjects. In addition, PD subjects displayed region-specific cortical atrophy in the left LOC and POC that were associated with increased diffusion measures over time. The finding of differential cortical gray and subcortical white matter associations between PD and healthy aging subjects was both unexpected and intriguing. The association between left

POC atrophy and increasing fractional anisotropy change (Figure 2) also is unexpected. Fractional anisotropy is the synthesized asymmetrical measure of the diffusion that occurs along all directions, and it is possible it represents a more complex biological process than radial and axial diffusivity. Thus, fractional anisotropy may depend on the stage of disease and timing of the measurements. Consistent with this hypothesis, fractional anisotropy values have been shown to increase and decrease over time in over the course of disease in multiple sclerosis patients (Calabrese et al., 2011; Ontaneda et al., 2014). Future studies, especially longitudinal follow-up in patients with different stages and durations of disease, are needed to confirm these findings and investigate underlying mechanisms.

4.4 Limitations & conclusions

Although our longitudinal design is a strength, the sample size is still relatively small. In designing the study, we tried to balance carefully the potential of both false positive and false negative results. To limit the probability of false positive gray-white matter associations, we only explored the associations in areas that were found to have lower gray matter volumes in PD subjects at baseline. To lower the likelihood of false negatives or excluding regions of potential interest, we utilized a criteria of raw $p < 0.05$ for areas to be included subsequently in the gray-white matter association analyses. Despite these efforts, it still is possible that we excluded some biologically meaningful regions of interest and/or introduced false positive regions of interest into the association analyses. It is important to point out, however, that 1) several of the reported gray-white matter associations at baseline survived correction for multiple comparisons and 2) the results of longitudinal analyses of radial and axial diffusivities were consistent with the baseline analysis.

Another limitation of the study is that we define white matter as total cerebral white matter or white matter underlying cortical subregions. This approach may lack sensitivity to assess the relationship between cortical gray matter and the white matter fibers that connect to it since several other fibers (i.e., long-range tracts not necessarily connected to the overlying cortex) are included and averaged in the same regions of interest. Future studies with tractography-based approaches to characterize white matter diffusion are needed. In this study, we utilized time-since-diagnosis as a surrogate for disease duration because time-of-first-symptom-onset could be vague and less precise than time-of-diagnosis. Further, poor white matter microstructure and white matter hyperintensities have been linked with cognitive impairment in PD (Agosta et al., 2014; Auning et al., 2014; Baggio et al., 2012; Debette and Markus, 2010; Kandiah et al., 2014; Koshimori et al., 2015; Mak et al., 2015; Shin et al., 2012; Sunwoo et al., 2014), and our exclusion criteria based on MMSE score limited our analysis to non-demented patients. Thus, future studies are warranted to determine whether different relationships between gray and white matter occur in subjects having PD with dementia. Lastly, we computed the rates of change over 36 months by calculating the slope over baseline, 18-, and 36-month visits. It is possible that the rates of change, however, could be non-linear as a function of time and further studies with even longer follow-up are needed. Nevertheless, the data are consistent with our overall conclusion that cortical gray and subcortical white matter are related in PD. Independent replication is needed, and may yield important information regarding the underlying mechanisms in normal aging and progressive neurodegenerative disease.

Supplementary Material

Refer to Web version on PubMed Central for supplementary material.

Acknowledgments

Study Funding:

NINDS (NS060722 and NS082151 to XH), the Hershey Medical Center GCRC (NIH M01RR10732), GCRC Construction Grant (C06RR016499), Pennsylvania Department of Health Tobacco CURE Funds, and the intramural research program of the NIH and the NIEHS.

We would like to express our gratitude to all of the participants who volunteered for this study. We acknowledge the MRI technical support of Mr. Jeffery Vesek, and the assistance of study coordinators Mss. Eleanore Hernandez, Brittany Jones, Melissa Santos, and Raghda Clayiff. We thank Professor Richard Mailman for suggestions regarding the preparation of this manuscript.

FUNDING

This study was funded by NINDS (NS060722 and NS082151 to XH), the Hershey Medical Center GCRC (NIH M01RR10732), GCRC Construction Grant (C06RR016499), and Pennsylvania Department of Health Tobacco CURE Funds.

References

- Abe O, Yamasue H, Aoki S, Suga M, Yamada H, Kasai K, Masutani Y, Kato N, Kato N, Ohtomo K. Aging in the CNS: comparison of gray/white matter volume and diffusion tensor data. *Neurobiol Aging*. 2008; 29(1):102–16. DOI: 10.1016/j.neurobiolaging.2006.09.003 [PubMed: 17023094]
- Agosta F, Canu E, Stefanova E, Sarro L, Tomic A, Spica V, Comi G, Kostic VS, Filippi M. Mild cognitive impairment in Parkinson's disease is associated with a distributed pattern of brain white matter damage. *Hum Brain Mapp*. 2014; 35(5):1921–9. DOI: 10.1002/hbm.22302 [PubMed: 23843285]
- Anderson MJ, Legendre P. An empirical comparison of permutation methods for tests of partial regression coefficients in a linear model. *Journal of Statistical Computation and Simulation*. 1999; 62(3):271–303. DOI: 10.1080/00949659908811936
- Aung WY, Mar S, Benzinger TL. Diffusion tensor MRI as a biomarker in axonal and myelin damage. *Imaging in medicine*. 2013; 5(5):427–40. [PubMed: 24795779]
- Auning E, Kjaervik VK, Selnes P, Aarsland D, Haram A, Bjoernerud A, Hessen E, Esnaashari A, Fladby T. White matter integrity and cognition in Parkinson's disease: a cross-sectional study. *BMJ Open*. 2014; 4(1):e003976.doi: 10.1136/bmjopen-2013-003976
- Avants BB, Epstein CL, Grossman M, Gee JC. Symmetric diffeomorphic image registration with cross-correlation: evaluating automated labeling of elderly and neurodegenerative brain. *Med Image Anal*. 2008; 12(1):26–41. S1361-8415(07)00060-6 [pii]; DOI: 10.1016/j.media.2007.06.004 [PubMed: 17659998]
- Baggio HC, Segura B, Ibarretxe-Bilbao N, Valldeoriola F, Marti MJ, Compta Y, Tolosa E, Junque C. Structural correlates of facial emotion recognition deficits in Parkinson's disease patients. *Neuropsychologia*. 2012; 50(8):2121–8. DOI: 10.1016/j.neuropsychologia.2012.05.020 [PubMed: 22640663]
- Bartzokis G, Beckson M, Lu PH, Nuechterlein KH, Edwards N, Mintz J. Age-related changes in frontal and temporal lobe volumes in men: a magnetic resonance imaging study. *Arch Gen Psychiatry*. 2001; 58(5):461–5. [PubMed: 11343525]
- Bates D, Maechler M, Bolker B, Walker S. Fitting Linear Mixed-Effects Models Using lme4. *Journal of Statistical Software*. 2015; 67(1):1–48. DOI: 10.18637/jss.v067.i01
- Benjamini Y, Hochberg Y. Controlling the false discovery rate: a practical and powerful approach to multiple testing. *Journal of the Royal Statistical Society Series B (Methodological)*. 1995:289–300.

- Bernal-Rusiel JL, Greve DN, Reuter M, Fischl B, Sabuncu MR. Statistical analysis of longitudinal neuroimage data with Linear Mixed Effects models. *NeuroImage*. 2013; 66:249260.doi: 10.1016/j.neuroimage.2012.10.065
- Bohnen NI, Albin RL. White matter lesions in Parkinson disease. *Nat Rev Neurol*. 2011; 7(4):229–36. DOI: 10.1038/nrneurol.2011.21 [PubMed: 21343896]
- Braak H, Bohl JR, Müller CM, Rüb U, de Vos RA, Del Tredici K. Stanley Fahn Lecture 2005: The staging procedure for the inclusion body pathology associated with sporadic Parkinson's disease reconsidered. *Movement disorders : official journal of the Movement Disorder Society*. 2006a; 21(12):2042–51. DOI: 10.1002/mds.21065 [PubMed: 17078043]
- Braak H, Del Tredici K, Rub U, de Vos RA, Jansen Steur EN, Braak E. Staging of brain pathology related to sporadic Parkinson's disease. *Neurobiol Aging*. 2003a; 24(2):197–211. [PubMed: 12498954]
- Braak H, Rub U, Schultz C, Del Tredici K. Vulnerability of cortical neurons to Alzheimer's and Parkinson's diseases. *J Alzheimers Dis*. 2006b; 9(3 Suppl):35–44.
- Braak H, Tredici K, Rüb U, de Vos R, Steur E, Braak E. Staging of brain pathology related to sporadic Parkinson's disease. *Neurobiology of Aging*. 2003b; 24(2)doi: 10.1016/S0197-4580(02)00065-9
- Buckner RL, Head D, Parker J, Fotenos AF, Marcus D, Morris JC, Snyder AZ. A unified approach for morphometric and functional data analysis in young, old, and demented adults using automated atlas-based head size normalization: reliability and validation against manual measurement of total intracranial volume. *Neuroimage*. 2004; 23(2):724–38. [PubMed: 15488422]
- Calabrese M, Rinaldi F, Seppi D, Favaretto A, Squarcina L, Mattisi I, Perini P, Bertoldo A, Gallo P. Cortical diffusion-tensor imaging abnormalities in multiple sclerosis: a 3-year longitudinal study. *Radiology*. 2011; 261(3):891–8. DOI: 10.1148/radiol.11110195 [PubMed: 22031708]
- Carrera E, Tononi G. Diaschisis: past, present, future. *Brain*. 2014; 137(Pt 9):2408–22. DOI: 10.1093/brain/awu101 [PubMed: 24871646]
- Chu Y, Kordower JH. The prion hypothesis of Parkinson's disease. *Curr Neurol Neurosci Rep*. 2015; 15(5):28.doi: 10.1007/s11910-015-0549-x [PubMed: 25868519]
- Debette S, Markus HS. The clinical importance of white matter hyperintensities on brain magnetic resonance imaging: systematic review and meta-analysis. *BMJ*. 2010; 341:c3666.doi: 10.1136/bmj.c3666 [PubMed: 20660506]
- Desikan RS, Ségonne F, Fischl B, Quinn BT, Dickerson BC, Blacker D, Buckner RL, Dale AM, Maguire RP, Hyman BT. An automated labeling system for subdividing the human cerebral cortex on MRI scans into gyral based regions of interest. *Neuroimage*. 2006; 31(3):968–80. [PubMed: 16530430]
- Dickstein DL, Kabaso D, Rocher AB, Luebke JI, Wearne SL, Hof PR. Changes in the structural complexity of the aged brain. *Aging Cell*. 2007; 6(3):275–84. DOI: 10.1111/j.1474-9726.2007.00289.x [PubMed: 17465981]
- Dubois B, Burn D, Goetz C, Aarsland D, Brown RG, Broe GA, Dickson D, Duyckaerts C, Cummings J, Gauthier S, Korczyn A, Lees A, Levy R, Litvan I, Mizuno Y, McKeith IG, Olanow CW, Poewe W, Sampaio C, Tolosa E, Emre M. Diagnostic procedures for Parkinson's disease dementia: recommendations from the movement disorder society task force. *Mov Disord*. 2007; 22(16):2314–24. DOI: 10.1002/mds.21844 [PubMed: 18098298]
- Duncan GW, Firbank MJ, Yarnall AJ, Khoo TK, Brooks DJ, Barker RA, Burn DJ, O'Brien JT. Gray and white matter imaging: A biomarker for cognitive impairment in early Parkinson's disease? *Mov Disord*. 2015; doi: 10.1002/mds.26312
- Fahn, S.; Elton, R. Unified Parkinson's disease rating scale. In: Fahn, S.; Jenner, P.; Marsden, CD.; Goldstein, M.; Calne, DB., editors. *Recent Developments in Parkinson's Disease*. Macmillan Healthcare Information; Florham Park, NJ: 1986.
- Fischl B, Dale AM. Measuring the thickness of the human cerebral cortex from magnetic resonance images. *Proc Natl Acad Sci U S A*. 2000; 97(20):11050–5. DOI: 10.1073/pnas.200033797 [PubMed: 10984517]
- Freedman D, Lane D. A nonstochastic interpretation of reported significance levels. *Journal of Business & Economic Statistics*. 1983; 1(4):292–8.

- Freeman SH, Kandel R, Cruz L, Rozkalne A, Newell K, Frosch MP, Hedley-Whyte ET, Locascio JJ, Lipsitz LA, Hyman BT. Preservation of neuronal number despite age-related cortical brain atrophy in elderly subjects without Alzheimer disease. *Journal of neuropathology and experimental neurology*. 2008; 67(12):1205–12. DOI: 10.1097/NEN.0b013e31818fc72f [PubMed: 19018241]
- Fukuda T, Takahashi J, Tanaka J. Tyrosine hydroxylase-immunoreactive neurons are decreased in number in the cerebral cortex of Parkinson's disease. *Neuropathology : official journal of the Japanese Society of Neuropathology*. 1999; 19(1):10–3. DOI: 10.1046/j.1440-1789.1999.00196.x [PubMed: 19519642]
- Gattellaro G, Minati L, Grisoli M, Mariani C, Carella F, Osio M, Ciceri E, Albanese A, Bruzzone MG. White matter involvement in idiopathic Parkinson disease: a diffusion tensor imaging study. *AJNR Am J Neuroradiol*. 2009; 30(6):1222–6. DOI: 10.3174/ajnr.A1556 [PubMed: 19342541]
- Goetz CG, Emre M, Dubois B. Parkinson's disease dementia: definitions, guidelines, and research perspectives in diagnosis. *Ann Neurol*. 2008a; 64(Suppl 2):S81–92. DOI: 10.1002/ana.21455 [PubMed: 19127578]
- Goetz CG, Tilley BC, Shaftman SR, Stebbins GT, Fahn S, Martinez-Martin P, Poewe W, Sampaio C, Stern MB, Dodel R, Dubois B, Holloway R, Jankovic J, Kulisevsky J, Lang AE, Lees A, Leurgans S, LeWitt PA, Nyenhuis D, Olanow CW, Rascol O, Schrag A, Teresi JA, van Hilten JJ, LaPelle N. Movement Disorder Society-sponsored revision of the Unified Parkinson's Disease Rating Scale (MDS-UPDRS): scale presentation and clinimetric testing results. *Mov Disord*. 2008b; 23(15):2129–70. DOI: 10.1002/mds.22340 [PubMed: 19025984]
- Gu Q, Huang P, Xuan M, Xu X, Li D, Sun J, Yu H, Wang C, Luo W, Zhang M. Greater loss of white matter integrity in postural instability and gait difficulty subtype of Parkinson's disease. *Can J Neurol Sci*. 2014; 41(6):763–8. DOI: 10.1017/cjn.2014.34 [PubMed: 25377626]
- Ham JH, Yun HJ, Sunwoo MK, Hong JY, Lee JM, Sohn YH, Lee PH. Topography of cortical thinning associated with white matter hyperintensities in Parkinson's disease. *Parkinsonism Relat Disord*. 2015; 21(4):372–7. DOI: 10.1016/j.parkreldis.2015.01.015 [PubMed: 25697488]
- Hamilton M. A rating scale for depression. *J Neurol Neurosurg Psychiatry*. 1960; 23:56–62. [PubMed: 14399272]
- Hattori T, Orimo S, Aoki S, Ito K, Abe O, Amano A, Sato R, Sakai K, Mizusawa H. Cognitive status correlates with white matter alteration in Parkinson's disease. *Human brain mapping*. 2012; 33(3):727–39. DOI: 10.1002/hbm.21245 [PubMed: 21495116]
- Huang P, Xu X, Gu Q, Xuan M, Yu X, Luo W, Zhang M. Disrupted white matter integrity in depressed versus non-depressed Parkinson's disease patients: a tract-based spatial statistics study. *J Neurol Sci*. 2014; 346(1–2):145–8. DOI: 10.1016/j.jns.2014.08.011 [PubMed: 25194633]
- Hughes AJ, Ben Shlomo Y, Daniel SE, Lees AJ. What features improve the accuracy of clinical diagnosis in Parkinson's disease: a clinicopathologic study. *Neurology*. 1992; 42(6):1142–6. [PubMed: 1603339]
- Hwang KS, Beyer MK, Green AE, Chung C, Thompson PM, Janvin C, Larsen JP, Aarsland D, Apostolova LG. Mapping cortical atrophy in Parkinson's disease patients with dementia. *J Parkinsons Dis*. 2013; 3(1):69–76. DOI: 10.3233/JPD-120151 [PubMed: 23938313]
- Ibarretxe-Bilbao N, Junque C, Segura B, Baggio HC, Marti MJ, Valldeoriola F, Bargallo N, Tolosa E. Progression of cortical thinning in early Parkinson's disease. *Mov Disord*. 2012; 27(14):1746–53. DOI: 10.1002/mds.25240 [PubMed: 23124622]
- Jernigan TL, Archibald SL, Fennema-Notestine C, Gamst AC, Stout JC, Bonner J, Hesselink JR. Effects of age on tissues and regions of the cerebrum and cerebellum. *Neurobiol Aging*. 2001; 22(4):581–94. [PubMed: 11445259]
- Ji L, Wang Y, Zhu D, Liu W, Shi J. White matter differences between multiple system atrophy (parkinsonian type) and Parkinson's disease: A diffusion tensor image study. *Neuroscience*. 2015; 305:109–16. DOI: 10.1016/j.neuroscience.2015.07.060 [PubMed: 26215920]
- Jiang H, He P, Adler CH, Shill H, Beach TG, Li R, Shen Y. Bid signal pathway components are identified in the temporal cortex with Parkinson disease. *Neurology*. 2012; 79(17):1767–73. DOI: 10.1212/WNL.0b013e3182703f76 [PubMed: 23019260]
- Johnson H, Harris G, Williams K. BRAINSFit: mutual information rigid registrations of whole-brain 3D images, using the insight toolkit. *Insight J*. 2007

- Joshi S, Davis B, Jomier M, Gerig G. Unbiased diffeomorphic atlas construction for computational anatomy. *Neuroimage*. 2004; 23(Suppl 1):S151–S60. [PubMed: 15501084]
- Kandiah N, Zainal NH, Narasimhalu K, Chander RJ, Ng A, Mak E, Au WL, Sitoh YY, Nadkarni N, Tan LC. Hippocampal volume and white matter disease in the prediction of dementia in Parkinson's disease. *Parkinsonism Relat Disord*. 2014; 20(11):1203–8. DOI: 10.1016/j.parkreldis.2014.08.024 [PubMed: 25258331]
- Klein A, Andersson J, Ardekani BA, Ashburner J, Avants B, Chiang MC, Christensen GE, Collins DL, Gee J, Hellier P, Song JH, Jenkinson M, Lepage C, Rueckert D, Thompson P, Vercauteren T, Woods RP, Mann JJ, Parsey RV. Evaluation of 14 nonlinear deformation algorithms applied to human brain MRI registration. *Neuroimage*. 2009; 46(3):786–802. DOI: 10.1016/j.neuroimage.2008.12.037 [PubMed: 19195496]
- Koshimori Y, Segura B, Christopher L, Lobaugh N, Duff-Canning S, Mizrahi R, Hamani C, Lang AE, Aminian K, Houle S, Strafella AP. Imaging changes associated with cognitive abnormalities in Parkinson's disease. *Brain structure & function*. 2015; 220(4):2249–61. DOI: 10.1007/s00429-014-0785-x [PubMed: 24816399]
- Lewis MM, Du G, Lee EY, Nasrallah Z, Sterlin NW, Zhang L, Wagner D, Kong L, Troster AI, Styner M, Eslinger PJ, Mailman RB, Huang X. The pattern of gray matter atrophy in Parkinson's disease differs in cortical and subcortical regions. *J Neurol*. 2016; 263(1):68–75. DOI: 10.1007/s00415-015-7929-7 [PubMed: 26486354]
- Liu Z, Wang Y, Gerig G, Gouttard S, Tao R, Fletcher T, Styner M. Quality Control of Diffusion Weighted Images. *Proceedings of SPIE--the International Society for Optical Engineering*. 2010; : 7628.doi: 10.1117/12.844748
- Mak E, Su L, Williams GB, O'Brien JT. Neuroimaging correlates of cognitive impairment and dementia in Parkinson's disease. *Parkinsonism Relat Disord*. 2015; 21(8):862–70. DOI: 10.1016/j.parkreldis.2015.05.013 [PubMed: 26004683]
- Marner L, Nyengaard JR, Tang Y, Pakkenberg B. Marked loss of myelinated nerve fibers in the human brain with age. *J Comp Neurol*. 2003; 462(2):144–52. DOI: 10.1002/cne.10714 [PubMed: 12794739]
- Nasreddine ZS, Phillips NA, Bedirian V, Charbonneau S, Whitehead V, Collin I, Cummings JL, Chertkow H. The Montreal Cognitive Assessment, MoCA: a brief screening tool for mild cognitive impairment. *J Am Geriatr Soc*. 2005; 53(4):695–9. JGS53221 [pii]; DOI: 10.1111/j.1532-5415.2005.53221.x [PubMed: 15817019]
- Oishi K, Faria A, Jiang H, Li X, Akhter K, Zhang J, Hsu JT, Miller MI, van Zijl PC, Albert M. Atlas-based whole brain white matter analysis using large deformation diffeomorphic metric mapping: application to normal elderly and Alzheimer's disease participants. *Neuroimage*. 2009; 46(2):486–99. [PubMed: 19385016]
- Ontaneda D, Sakaie K, Lin J, Wang X, Lowe MJ, Phillips MD, Fox RJ. Identifying the start of multiple sclerosis injury: a serial DTI study. *Journal of neuroimaging : official journal of the American Society of Neuroimaging*. 2014; 24(6):569–76. DOI: 10.1111/jon.12082 [PubMed: 25370339]
- Orimo S, Uchihara T, Kanazawa T, Itoh Y, Wakabayashi K, Kakita A, Takahashi H. Unmyelinated axons are more vulnerable to degeneration than myelinated axons of the cardiac nerve in Parkinson's disease. *Neuropathol Appl Neurobiol*. 2011; 37(7):791–802. DOI: 10.1111/j.1365-2990.2011.01194.x [PubMed: 21696416]
- Pereira JB, Svenningsson P, Weintraub D, Bronnick K, Lebedev A, Westman E, Aarsland D. Initial cognitive decline is associated with cortical thinning in early Parkinson disease. *Neurology*. 2014; 82(22):2017–25. WNL.000000000000483 [pii]; DOI: 10.1212/WNL.000000000000483 [PubMed: 24808018]
- R_Core_Team. R: A language and environment for statistical computing. R Foundation for Statistical Computing; Vienna, Austria: 2016.
- Rakic P. Specification of cerebral cortical areas. *Science*. 1988; 241(4862):170–6. [PubMed: 3291116]
- Rakic P. Radial versus tangential migration of neuronal clones in the developing cerebral cortex. *Proc Natl Acad Sci U S A*. 1995; 92(25):11323–7. [PubMed: 8524778]

- Ramirez-Ruiz B, Marti MJ, Tolosa E, Gimenez M, Bargallo N, Valldeoriola F, Junque C. Cerebral atrophy in Parkinson's disease patients with visual hallucinations. *Eur J Neurol*. 2007; 14(7):750–6. DOI: 10.1111/j.1468-1331.2007.01768.x [PubMed: 17594330]
- Reuter M, Fischl B. Avoiding asymmetry-induced bias in longitudinal image processing. *Neuroimage*. 2011; 57(1):19–21. S1053-8119(11)00253-9 [pii]; DOI: 10.1016/j.neuroimage.2011.02.076 [PubMed: 21376812]
- Ribeiro PF, Ventura-Antunes L, Gabi M, Mota B, Grinberg LT, Farfel JM, Ferretti-Rebustini RE, Leite RE, Filho JW, Herculano-Houzel S. The human cerebral cortex is neither one nor many: neuronal distribution reveals two quantitatively different zones in the gray matter, three in the white matter, and explains local variations in cortical folding. *Frontiers in neuroanatomy*. 2013;7. [PubMed: 23717265]
- Rizzo G, Martinelli P, Manners D, Scaglione C, Tonon C, Cortelli P, Malucelli E, Capellari S, Testa C, Parchi P, Montagna P, Barbiroli B, Lodi R. Diffusion-weighted brain imaging study of patients with clinical diagnosis of corticobasal degeneration, progressive supranuclear palsy and Parkinson's disease. *Brain*. 2008; 131(Pt 10):2690–700. DOI: 10.1093/brain/awn195 [PubMed: 18819991]
- Salvador R, Pena A, Menon DK, Carpenter TA, Pickard JD, Bullmore ET. Formal characterization and extension of the linearized diffusion tensor model. *Hum Brain Mapp*. 2005; 24(2):144–55. DOI: 10.1002/hbm.20076 [PubMed: 15468122]
- Scheibel ME, Lindsay RD, Tomiyasu U, Scheibel AB. Progressive dendritic changes in aging human cortex. *Exp Neurol*. 1975; 47(3):392–403. [PubMed: 48474]
- Segura B, Baggio HC, Marti MJ, Valldeoriola F, Compta Y, Garcia-Diaz AI, Vendrell P, Bargallo N, Tolosa E, Junque C. Cortical thinning associated with mild cognitive impairment in Parkinson's disease. *Mov Disord*. 2014; 29(12):1495–503. DOI: 10.1002/mds.25982 [PubMed: 25100674]
- Seo SW, Lee JM, Im K, Park JS, Kim SH, Kim ST, Ahn HJ, Chin J, Cheong HK, Weiner MW, Na DL. Cortical thinning related to periventricular and deep white matter hyperintensities. *Neurobiol Aging*. 2012; 33(7):1156–67. DOI: 10.1016/j.neurobiolaging.2010.12.003 [PubMed: 21316813]
- Sexton CE, Walhovd KB, Storsve AB, Tamnes CK, Westlye LT, Johansen-Berg H, Fjell AM. Accelerated changes in white matter microstructure during aging: a longitudinal diffusion tensor imaging study. *J Neurosci*. 2014; 34(46):15425–36. DOI: 10.1523/JNEUROSCI.0203-14.2014 [PubMed: 25392509]
- Shin J, Choi S, Lee JE, Lee HS, Sohn YH, Lee PH. Subcortical white matter hyperintensities within the cholinergic pathways of Parkinson's disease patients according to cognitive status. *J Neurol Neurosurg Psychiatry*. 2012; 83(3):315–21. DOI: 10.1136/jnnp-2011-300872 [PubMed: 22228726]
- Singh, I. *Textbook of Human Neuroanatomy*. Jaypee Brothers; 2006.
- Song SK, Sun SW, Ramsbottom MJ, Chang C, Russell J, Cross AH. Demyelination revealed through MRI as increased radial (but unchanged axial) diffusion of water. *Neuroimage*. 2002; 17(3):1429–36. [PubMed: 12414282]
- Song SK, Lee JE, Park HJ, Sohn YH, Lee J, Lee P. The pattern of cortical atrophy in patients with Parkinson's disease according to cognitive status. *Movement Disorders*. 2011; doi: 10.1002/mds.23477
- Song SK, Yoshino J, Le TQ, Lin SJ, Sun SW, Cross AH, Armstrong RC. Demyelination increases radial diffusivity in corpus callosum of mouse brain. *Neuroimage*. 2005; 26(1):132–40. DOI: 10.1016/j.neuroimage.2005.01.028 [PubMed: 15862213]
- Storsve AB, Fjell AM, Tamnes CK, Westlye LT, Overbye K, Aasland HW, Walhovd KB. Differential longitudinal changes in cortical thickness, surface area and volume across the adult life span: regions of accelerating and decelerating change. *J Neurosci*. 2014; 34(25):8488–98. DOI: 10.1523/JNEUROSCI.0391-14.2014 [PubMed: 24948804]
- Sunwoo MK, Jeon S, Ham JH, Hong JY, Lee JE, Lee JM, Sohn YH, Lee PH. The burden of white matter hyperintensities is a predictor of progressive mild cognitive impairment in patients with Parkinson's disease. *Eur J Neurol*. 2014; 21(6):922–e50. DOI: 10.1111/ene.12412 [PubMed: 24661277]

- Terry RD, DeTeresa R, Hansen LA. Neocortical cell counts in normal human adult aging. *Annals of neurology*. 1987; 21(6):530–9. [PubMed: 3606042]
- Tinaz S, Courtney MG, Stern CE. Focal cortical and subcortical atrophy in early Parkinson's disease. *Mov Disord*. 2011; 26(3):436–41. DOI: 10.1002/mds.23453 [PubMed: 21462259]
- Tomlinson CL, Stowe R, Patel S, Rick C, Gray R, Clarke CE. Systematic review of levodopa dose equivalency reporting in Parkinson's disease. *Mov Disord*. 2010; 25(15):2649–53. DOI: 10.1002/mds.23429 [PubMed: 21069833]
- Tsukamoto K, Matsusue E, Kanasaki Y, Kakite S, Fujii S, Kaminou T, Ogawa T. Significance of apparent diffusion coefficient measurement for the differential diagnosis of multiple system atrophy, progressive supranuclear palsy, and Parkinson's disease: evaluation by 3.0-T MR imaging. *Neuroradiology*. 2012; 54(9):947–55. DOI: 10.1007/s00234-012-1009-9 [PubMed: 22274571]
- Westlye LT, Walhovd KB, Dale AM, Bjornerud A, Due-Tønnessen P, Engvig A, Grydeland H, Tamnes CK, Ostby Y, Fjell AM. Life-span changes of the human brain white matter: diffusion tensor imaging (DTI) and volumetry. *Cereb Cortex*. 2010; 20(9):2055–68. DOI: 10.1093/cercor/bhp280 [PubMed: 20032062]
- Winkler AM, Kochunov P, Blangero J, Almasy L, Zilles K, Fox PT, Duggirala R, Glahn DC. Cortical thickness or grey matter volume? The importance of selecting the phenotype for imaging genetics studies. *Neuroimage*. 2010; 53(3):1135–46. DOI: 10.1016/j.neuroimage.2009.12.028 [PubMed: 20006715]
- Worker A, Blain C, Jarosz J, Chaudhuri KR, Barker GJ, Williams SC, Brown RG, Leigh PN, Dell'Acqua F, Simmons A. Diffusion tensor imaging of Parkinson's disease, multiple system atrophy and progressive supranuclear palsy: a tract-based spatial statistics study. *PLoS One*. 2014; 9(11):e112638.doi: 10.1371/journal.pone.0112638 [PubMed: 25405990]
- Zhang Y, Zhang J, Xu J, Wu X, Zhang Y, Feng H, Wang J, Jiang T. Cortical gyrification reductions and subcortical atrophy in Parkinson's disease. *Mov Disord*. 2014; 29(1):122–6. DOI: 10.1002/mds.25680 [PubMed: 24123500]

HIGHLIGHTS

- Gray and white matter degeneration have been documented in PD.
- The relationship of gray and white matter in PD is unknown.
- Cortical gray matter atrophy may be related to white matter properties in PD.
- These associations are not observed in a healthy aging population.

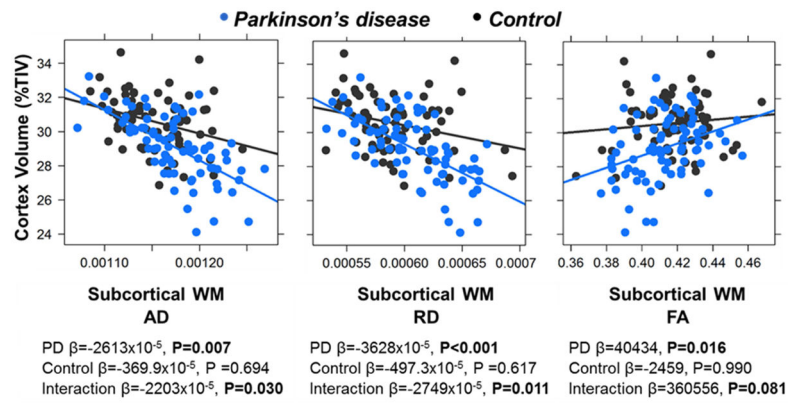


Figure 1. Relationships between cortical gray matter volume and underlying subcortical white matter diffusion in PD vs. Controls at baseline

Cortex gray matter volumes are shown as a percent of intracranial volume for illustration purposes. Figures show regression coefficients for PD and control subjects for the correlations between cortex volume and subcortical white matter diffusion measures axial diffusion (AD), radial diffusion (RD), and fractional anisotropy (FA). Bolded p values represent significant correlations after Bonferroni correction for multiple comparisons ($p = 0.017$). Abbreviations: PD = Parkinson's disease, WM = white matter.

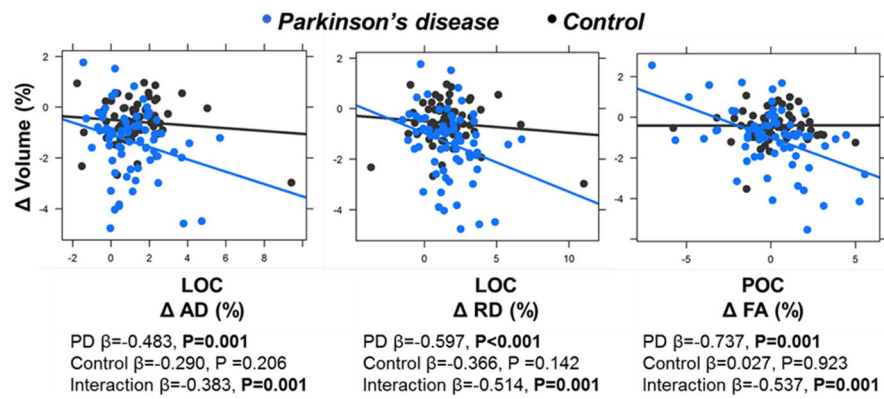


Figure 2. Relationship between change in left lateral occipital (LOC) and change in diffusion measures axial diffusion (AD) and radial diffusion (RD), and in left posterior occipital cortex (POC) and fractional anisotropy (FA) in PD vs. Controls using longitudinal data

Figures show regression coefficients for PD and control subjects for the correlations between change in LOC volume and change in diffusion measures axial diffusion (AD) and radial diffusion (RD), and POC volume and fractional anisotropy (FA). Bolded p values represent significant correlations after Bonferroni correction for multiple comparisons ($p < 0.017$). PD subjects showed decreased AD and RD values with decreasing LOC volume, and decreased FA values with decreasing POC volume. The changes in Controls were not significant.

Table 1

Baseline and follow-up demographic and clinical characteristics of study subjects.

	PD	Control	P-Value
N, Baseline (Female:Male)	76 (29:47)	70 (36:34)	0.134
N, 18 months (Female:Male)	62 (27:35)	60 (31:30)	0.472
N, 36 months (Female:Male)	50 (24:26)	56 (30:26)	0.697
Age (years)	63.3 ± 8.4	59.9 ± 7.7	0.011
Education (years)	15.9 ± 2.7	16.6 ± 2.8	0.135
MMSE	29.1 ± 1.1	29.5 ± 0.9	0.024
MoCA	24.6 ± 3.6	26.1 ± 2.5	0.007
HAM	7.7 ± 4.5	3.8 ± 2.5	<0.0001
UPDRS-III	22.5 ± 14.3	-	-
LEDD	557 ± 457	-	-
Duration of disease (years)	4.9 ± 5.5	-	-
HY Stage	1.8 ± 0.7	-	-

Abbreviations – HAM: Hamilton depression rating scale; HY: Hoehn-Yahr; LEDD: levodopa daily equivalent dosage; MMSE: Mini mental state exam; MoCA: Montreal Cognitive Assessment; UPDRS: Unified Parkinson's disease rating scale;

Table 2

Areas of cortical gray matter volumes that were significantly different between Parkinson's and control subjects at baseline (least squares adjusted means) and corresponding rates of change (model estimates).

	Comparisons of GM Volume (mm ³)			Comparisons of GM Volume (mm ³ /y)		
	PD	Control	P-Value	PD	Control	P-Value
Cortex Total	446477 ± 33247	458554 ± 34885	0.006	-63371 ± 4828	-61552 ± 2314	0.001*
Left IT	10167 ± 1650	10691 ± 1731	0.015	-65.0 ± 159.3	-33.2 ± 70.7	0.055
Left LOC	11157 ± 1894	11838 ± 1987	0.007	-73.5 ± 158.9	-14.0 ± 63.6	0.002*
Left MT	9916 ± 1725	10640 ± 1810	0.002*	-74.8 ± 146.7	-21.1 ± 73.2	0.001*
Left PoC	9509 ± 1355	10137 ± 1421	0.001*	-97.6 ± 126.9	-56.9 ± 80.6	0.025
Right BSTS	2144 ± 491	2308 ± 515	0.012	-18.8 ± 36.3	-13.6 ± 17.0	0.202
Right Fus	9232 ± 1650	9759 ± 1732	0.018	-79.6 ± 109.7	-40.3 ± 85.1	0.012*
Right IP	13676 ± 2437	14561 ± 2557	0.006*	-90.0 ± 226.3	-18.7 ± 107.1	0.008*
Right IT	9907 ± 1780	10854 ± 1868	<0.001*	-67.9 ± 132.4	-34.6 ± 66.4	0.029
Right LOF	6943 ± 821	7222 ± 862	0.011	-48.8 ± 82.6	-23.5 ± 66.3	0.021
Right MT	11027 ± 1743	11732 ± 1829	0.002*	-86.1 ± 125.5	-39.5 ± 71.1	0.004*
Right PoC	9130 ± 1540	9570 ± 1616	0.035	-78.0 ± 149.3	-44.2 ± 92.2	0.090
Right SP	12576 ± 1905	13247 ± 1999	0.011	-128.0 ± 221.6	-76.3 ± 135.1	0.069

Bold denotes p-values <0.05 without adjusting multiple comparisons.

* Significant after false discovery rate adjustment using 70 cortical regions

Abbreviations – AD: Axial diffusivity; BST: Banks of superior temporal sulcus; Fus: Fusiform; IP: Inferior parietal; IT: Inferior temporal; L: Left; LOC: Lateral occipital; LOF: Lateral orbitofrontal; MT: Middle temporal; PoC: Postcentral; RD: Radial diffusivity; R: Right; SP: Superior parietal;

Table 3

Comparisons of baseline subcortical white matter diffusivities and their annual changes between Parkinson's and control subjects.

	Group Comparisons											
	AD ($\times 10^{-5}$ mm ² /sec)			RD ($\times 10^{-5}$ mm ² /sec)			FA					
	PD	Control	P-Val	PD	Control	P-Val	PD	Control	P-Val	PD	Control	P-Val
Overall	116.8 ± 4.2	116.1 ± 4.4	0.262	60.1 ± 3.9	59.6 ± 4.0	0.304	0.41 ± 0.02	0.42 ± 0.025	0.67			
Subregions												
L. IT	112.9 ± 6.3	111.4 ± 6.6	0.088	63.5 ± 5.2	62.6 ± 5.4	0.154	0.39 ± 0.04	0.40 ± 0.04	0.53			
L. LOC	93.7 ± 7.0	92.3 ± 7.4	0.138	63.9 ± 5.8	62.9 ± 6.1	0.177	0.36 ± 0.04	0.36 ± 0.05	0.79			
L. MT	107.0 ± 5.6	105.6 ± 5.9	0.052	61.5 ± 4.9	60.0 ± 5.1	0.026	0.41 ± 0.04	0.41 ± 0.04	0.11			
L. PoC	103.5 ± 6.4	102.2 ± 6.7	0.116	61.9 ± 5.6	61.1 ± 5.8	0.317	0.39 ± 0.04	0.39 ± 0.05	0.85			
R. BSTS	109.7 ± 6.5	107.5 ± 6.8	0.011	64.7 ± 5.7	63.0 ± 6.0	0.023	0.37 ± 0.04	0.38 ± 0.04	0.30			
R. Fus	97.2 ± 6.6	95.7 ± 7.0	0.081	69.3 ± 5.4	68.0 ± 5.6	0.066	0.32 ± 0.03	0.32 ± 0.03	0.34			
R. IP	103.5 ± 7.6	102.6 ± 8.0	0.383	64.6 ± 8.1	63.3 ± 8.5	0.219	0.37 ± 0.05	0.38 ± 0.05	0.36			
R. IT	116.1 ± 8.4	114.5 ± 8.8	0.147	69.1 ± 6.3	67.5 ± 6.6	0.057	0.37 ± 0.04	0.38 ± 0.04	0.17			
R. LOF	98.5 ± 5.6	98.8 ± 5.9	0.665	66.1 ± 5.2	66.1 ± 5.5	0.950	0.32 ± 0.03	0.32 ± 0.04	0.91			
R. MT	111.1 ± 7.4	109.5 ± 7.8	0.116	65.7 ± 5.6	63.8 ± 5.9	0.011	0.38 ± 0.03	0.39 ± 0.03	0.06			
R. PoC	103.5 ± 6.4	102.2 ± 6.7	0.112	61.9 ± 5.6	61.1 ± 5.8	0.313	0.39 ± 0.04	0.39 ± 0.05	0.85			
R. SP	110.7 ± 9.6	109.5 ± 10.1	0.359	62.5 ± 8.8	60.8 ± 9.3	0.158	0.42 ± 0.05	0.43 ± 0.05	0.34			
	AD ($\times 10^{-5}$ mm ² /sec)/y			RD ($\times 10^{-5}$ mm ² /sec)/y			FA ($\times 10^{-3}$)/y					
Overall	0.954 ± 0.639	0.976 ± 0.412	0.868	0.789 ± 0.603	0.599 ± 0.329	0.059	-2.2 ± 4.1	-0.6 ± 3.1	0.018			
Subregions												

	Group Comparisons											
	AD ($\times 10^{-5}$ mm ² /sec)			RD ($\times 10^{-5}$ mm ² /sec)			FA					
	PD	Control	P-Val	PD	Control	P-Val	PD	Control	P-Val	PD	Control	P-Val
L. IT	0.288 ± 0.738	0.129 ± 0.850	0.314	0.483 ± 0.829	0.312 ± 0.676	0.279	-2.4 ± 4.9	-1.5 ± 3.5	0.381			
L. LOF	1.062 ± 0.985	1.287 ± 0.780	0.235	0.870 ± 0.847	0.777 ± 0.655	0.535	-1.5 ± 5.6	0.4 ± 4.9	0.009			
L. MT	0.549 ± 0.814	0.505 ± 0.767	0.763	0.652 ± 0.833	0.542 ± 0.556	0.424	-2.0 ± 5.2	-1.0 ± 4.9	0.226			
L. PoC	1.251 ± 0.900	1.130 ± 0.488	0.403	0.923 ± 0.872	0.617 ± 0.579	0.015	-1.1 ± 8.1	1.4 ± 5.5	0.023			
R. BSTS	1.056 ± 1.065	1.230 ± 1.001	0.443	0.699 ± 0.994	0.803 ± 0.913	0.596	-0.7 ± 5.5	-0.5 ± 6.8	0.812			
R. Fus	0.538 ± 0.953	0.770 ± 0.710	0.297	0.486 ± 0.791	0.493 ± 0.563	0.966	-0.9 ± 3.2	0.6 ± 3.6	0.017			
R. IP	1.342 ± 0.798	1.400 ± 0.835	0.761	0.944 ± 0.779	0.928 ± 0.806	0.925	-1.1 ± 4.4	-0.2 ± 3.9	0.293			
R. IT	0.812 ± 1.095	1.063 ± 0.832	0.262	0.925 ± 0.723	0.860 ± 0.677	0.679	-3.5 ± 4.1	-2.0 ± 4.6	0.026			
R. LOF	1.182 ± 1.717	1.124 ± 0.838	0.781	1.079 ± 1.540	0.841 ± 0.535	0.148	-1.9 ± 4.1	-0.1 ± 2.0	0.004			
R. MT	0.721 ± 1.080	0.922 ± 0.840	0.323	0.835 ± 0.958	0.758 ± 0.751	0.599	-3.1 ± 5.3	-1.6 ± 4.7	0.036			
R. PoC	1.295 ± 1.025	1.349 ± 0.581	0.742	0.861 ± 0.934	0.760 ± 0.687	0.476	-0.2 ± 6.9	1.4 ± 5.6	0.269			
R. SP	1.623 ± 1.025	1.709 ± 0.987	0.700	1.343 ± 0.918	1.298 ± 0.789	0.808	-4.0 ± 6.5	-2.9 ± 4.0	0.325			

Bold denotes raw p values <0.05 without adjusting for multiple comparisons

Abbreviations – AD: Axial diffusivity; BST: Banks of superior temporal sulcus; Fus: Fusiform; IP: Inferior parietal; IT: Inferior temporal; L: Left; LOF: Lateral occipital; LOF: Lateral occipital; MT: Middle temporal; PoC: Postcentral; RD: Radial diffusivity; R: Right; SP: Superior parietal;

Table 4

Associations between cortical gray matter volumes and diffusion measurements in underlying white matter at baseline.

	PD Subjects						Control Subjects					
	AD		RD		FA		AD		RD		FA	
	$\beta \times 10^{-5}$	P-Val	$\beta \times 10^{-5}$	P-Val	β	P-Val	$\beta \times 10^{-5}$	P-Val	$\beta \times 10^{-5}$	P-Val	β	P-Val
Cortex Total	-2613	0.007*	-3628	< 0.001*	40434	0.016*	-369.9	0.694	-497.3	0.617	-2459	0.990
Subregions												
L. IT	-6.1	0.845	-42.4	0.220	4722	0.345	-6.6	0.852	-62.4	0.160	7966	0.284
L. LOC	-83.9	0.013	-88.2	0.022	9394	0.136	29.4	0.336	8.2	0.840	5997	0.426
L. MT	-13.9	0.683	-76.7	0.044	11869	0.020	12.9	0.774	-47.2	0.341	11230	0.082
L. PoC	-17.9	0.468	-48.3	0.099	7908	0.063	8.0	0.767	7.8	0.802	-2314	0.583
R. BSTS	-1.4	0.891	0.3	0.977	81	0.954	1.2	0.899	8.2	0.523	-2198	0.287
R. Fus	-17.5	0.465	-28.7	0.328	1188	0.887	-37.0	0.414	-61.9	0.301	-3751	0.718
R. IP	-71.5	0.040	-80.5	0.030	9486	0.230	-41.7	0.317	-58.0	0.083	9353	0.175
R. IT	4.5	0.859	-25.7	0.380	8451	0.183	6.4	0.831	3.6	0.930	3325	0.673
R. LOF	11.9	0.533	-11.8	0.551	5130	0.153	18.3	0.254	-4.9	0.771	5961	0.053
R. MT	-58.4	0.067	-66.0	0.102	9877	0.167	61.3	0.020	43.1	0.229	7919	0.222
R. PoC	-59.5	0.025	-101.8	0.001#	9293	0.048	-2.7	0.933	-17.5	0.606	2695	0.585
R. SP	-3.4	0.866	-3.2	0.882	-201	0.973	-2.2	0.944	4.4	0.883	-2001	0.700

Estimates and p-values in are calculated using a linear model with Parkinson's and control subjects.

Bold denotes unadjusted $p < 0.05$.

* Significant after Bonferroni correction with three diffusion measurements for main hypotheses testing of overall cortical and subcortical regions ($p = 0.017$)

Significant after Bonferroni correction for exploration of 12 subregions and three diffusion measurements ($p = 0.0013$).

Abbreviations – AD: Axial diffusivity; BST: Banks of superior temporal sulcus; Fus: Fusiform; IP: Inferior parietal; IT: Inferior temporal; L: Left; LOC: Lateral occipital; LOF: Lateral orbitofrontal; MT: Middle temporal; PoC: Postcentral; RD: Radial diffusivity; R: Right; SP: Superior parietal =

Table 5
Associations between annual change in cortical gray matter volume and diffusion of underlying white matter.

	PD Subjects						Control Subjects					
	AD		RD		FA		AD		RD		FA	
	β	P-Val	β	P-Val	β	P-Val	β	P-Val	β	P-Val	β	P-Val
Cortex Total	-0.162	0.084	-0.005	0.969	-0.289	0.030	0.119	0.488	0.209	0.420	-0.150	0.490
Subregions												
L. IT	-0.110	0.241	-0.164	0.246	-0.003	0.983	0.360	0.033	0.499	0.074	-0.300	0.347
L. LOC	-0.483	<0.001#	-0.597	<0.001#	0.161	0.395	-0.290	0.206	-0.366	0.142	0.053	0.835
L. MT	-0.129	0.070	-0.094	0.464	-0.184	0.202	-0.071	0.646	0.064	0.801	-0.194	0.476
L. PoC	-0.101	0.315	0.177	0.165	-0.737	<0.001#	0.155	0.326	0.114	0.593	0.027	0.923
R. BSTS	0.047	0.686	0.172	0.297	-0.283	0.125	0.257	0.196	0.171	0.462	0.139	0.574
R. Fus	-0.090	0.600	-0.037	0.828	-0.211	0.323	-0.034	0.844	-0.149	0.460	0.216	0.421
R. IP	-0.103	0.364	-0.024	0.874	-0.251	0.089	0.318	0.042	0.644	0.006	-0.582	0.004
R. IT	-0.038	0.776	0.093	0.555	-0.287	0.050	0.054	0.841	0.232	0.503	-0.430	0.127
R. LOF	0.407	0.046	0.337	0.202	0.012	0.961	-0.006	0.972	-0.003	0.987	-0.188	0.304
R. MT	-0.015	0.922	0.196	0.258	-0.413	0.018	0.192	0.463	0.095	0.780	0.003	0.991
R. PoC	-0.003	0.973	0.160	0.179	-0.444	0.012	0.138	0.282	0.190	0.270	-0.116	0.618
R. SP	-0.263	0.014	-0.190	0.206	-0.262	0.082	0.255	0.059	0.438	0.022	-0.401	0.010

Estimates and p-values in are calculated using a linear model with Parkinson's and control subjects.

Bold denotes unadjusted $p < 0.05$.

Significant after Bonferroni correction for exploration of 12 subregions and three diffusion measurements ($p < 0.0013$).

Abbreviations – AD: Axial diffusivity; BST: Banks of superior temporal sulcus; Fus: Fusiform; IP: Inferior parietal; IT: Inferior temporal; L: Left; LOC: Lateral occipital; LOF: Lateral orbitofrontal; MT: Middle temporal; PoC: Postcentral; RD: Radial diffusivity; R: Right; SP: Superior parietal